

Study of Shock Fronts and Solitary Profiles in a Weak Relativistic Plasma and its Evolution into an Amplitude Modulated Envelope Soliton

Ahona Majumdar¹, Anusree Sen¹, Biswasaran Panda¹, Ritwik Ghosal¹, Sweta Mallick¹ and S Chandra^{2*}

¹*Department of Physics, St. Xavier's College (Autonomous), Kolkata*

²*Department of Physics, Government General Degree College, Kushmandi, India 733121*

**Institute of Natural Sciences and Applied Technology, Kolkata, India, 700032*

E-mail: biswasaranpanda78@gmail.com (corresponding author)

We have studied, the linear and non-linear properties of shocks and solitary structures of ion acoustic and electrostatic waves in a two-component electron-ion dense quantum plasma, by using reductive perturbation technique. Here, we have neglected collisions of the ions and electrons. The shocks arise due to viscous force. Here we have derived the KdV-Burgers equation with the help of standard reductive perturbation technique and analysed it numerically. For electrostatic wave, we have dealt in the quantum realm and studied the dispersion curves, shock fronts and solitary profiles. By using the standard method of multiple scale perturbation technique, a non-linear Schrodinger equation containing quantum effects is derived. The KdVB equation is transformed to the corresponding NLSE developing non-linear wave-packets called envelope solitons. In this paper we have also discussed time evolution of the solution of a forced KdV equation.

1. Introduction

Plasma is the fourth state of matter. Plasma waves can be in electrostatic, ion acoustic or dust acoustic mode. We will restrict ourselves to the discussion of electrostatic and ion acoustic modes [1]. The basic difference between the two modes mentioned above is that electrostatic mode depends only on the mass of the electrons, the ions are assumed to be infinitely massive i.e. stationary and ion acoustic mode [10] the dependence is on the ion mass but the electrons are assumed to be massless and to re-distribute themselves according to the Boltzmann relation. Most of the works on electron acoustic waves are for classical non-relativistic plasma [2]. For some compact astrophysical objects like the gravitational collapse of dying stars, formation of white dwarfs and neutron stars exist in extreme condition of density [9]. All these works use quantum hydrodynamic models and consider weakly-relativistic aspects. But in extreme conditions of density, such as in a typical astrophysical aspect, the degeneracy can be relativistic. Here, both quantum and relativistic effects may play a vital role. The purpose of this paper is to investigate the linear and nonlinear properties of electrostatic and ion-acoustic mode in QHD plasma consisting of weakly relativistic degenerate electrons and stationary ions [3]. Rogue Waves are unexpectedly high amplitude and highly energetic single wave, which appear both in the open ocean and in coastal areas. Here we check the stability of the rogue waves from the

NLSE [4]. We may find that KdV or KdV-type solitons, under an external periodic force are often termed as forced KdV solitons [5]. Then, we study the solitary structure in presence of external periodic force and the temporal behaviour under the influence of the external force [6]. This provides perfect agreement with the basic understanding of nonlinear behaviour in plasmas. Then we have tried to explain the observations [7][8] in plasma tail with our theoretical results.

2. Basic Formulations

In order to study the ion-acoustic and electro-static modes in such a plasma, we start with the set of normalised equations:

$$\frac{\partial \bar{n}_e}{\partial \bar{t}} + \frac{\partial}{\partial \bar{x}} (\bar{n}_e \bar{u}_e) = 0 \quad (1)$$

$$\frac{\partial \bar{n}_i}{\partial \bar{t}} + \frac{\partial}{\partial \bar{x}} (\bar{n}_i \bar{u}_i) = 0 \quad (2)$$

$$\left(\frac{\partial}{\partial \bar{t}} + \bar{u}_i \frac{\partial}{\partial \bar{x}} \right) \bar{u}_i = -\mu \frac{\partial \bar{\phi}}{\partial \bar{x}} + \bar{n}_i \frac{\partial^2 \bar{u}_i}{\partial \bar{x}^2} \quad (3)$$

$$0 = \frac{\partial \bar{\phi}}{\partial \bar{x}} - A n_e^{-\frac{1}{3}} \frac{\partial \bar{n}_e}{\partial \bar{x}} + \frac{H^2}{2} \frac{\partial}{\partial \bar{x}} \left[\frac{1}{\sqrt{\bar{n}_e}} \frac{\partial^2 \sqrt{\bar{n}_e}}{\partial \bar{x}^2} \right] \quad (4)$$

$$\frac{\partial^2 \bar{\phi}}{\partial \bar{x}^2} = \bar{n}_e - \bar{n}_i \quad (5)$$

Where $A = \frac{1}{12} \left(\frac{3}{\pi} \right)^{\frac{2}{3}} \frac{\hbar^2}{2m_e} \left(\frac{1}{2K_B T_{Fe}} \right)$

One dimensional quantum diffraction parameter H is defined as $H = \frac{\hbar \omega_{pe}}{2K_B T_{Fe}}$ where $\omega_{pe} = \left(\frac{4\pi n_{e0} e^2}{m_e} \right)^{\frac{1}{2}}$

For, electrostatic wave, We use the equations (1) to (5) which deal with both ions and electrons for further linear and non-linear study. Similarly for ion acoustic wave, The electrons are assumed to have infinite mass and they are considered stationary. Only ions are mobile. So, we use only the equations (2) (3) and (5) which are devoid of electrons.

Here, we have used the following normalization scheme,

$$n_i \rightarrow \frac{n_i}{n_0} ; u_i \rightarrow \frac{u_i}{u_0} ; t \rightarrow \frac{t}{\omega_p} ; x \rightarrow \frac{x \omega_p}{V_{Fe}} ;$$

$$\varphi \rightarrow \frac{\varphi}{2K_B T} ; \omega_p \rightarrow \sqrt{\frac{4\pi n_0 e^2}{m_e}} ; \eta \rightarrow \frac{\eta \omega_p}{V_{Fe}^2 m_e} ;$$

$$V_{Fe} \rightarrow \sqrt{\frac{2K_B T}{m_e}}$$

3. Analytical Studies

From the equations (1) to (5) discussed above, we have obtained the following dispersion relations which describes the effect of dispersion on the properties of any propagating wave in the plasma medium. It provides a relation between k and ω . In the normalized equations we have a viscous force which is a dissipative term. So, there will be an imaginary part in the dispersion relation which corresponds to attenuation of the wave. Also, there is a real part which corresponds to free propagation of the wave. So, the propagation wave number, k , is given by, $k = k_r + i k_i$.

Using the perturbation,

$$\begin{bmatrix} n_j \\ u_j \\ \varphi \end{bmatrix} = \begin{bmatrix} 1 \\ u_0 \\ \varphi_0 \end{bmatrix} + \delta \begin{bmatrix} n_j^{(1)} \\ u_j^{(1)} \\ \varphi^{(1)} \end{bmatrix} + \delta^2 \begin{bmatrix} n_j^{(2)} \\ u_j^{(2)} \\ \varphi^{(2)} \end{bmatrix} + \dots \quad (6)$$

Where, δ is a very small parameter. From the linear analysis we have derive the following dispersion relations,

a) In ion-acoustic mode:

$$\omega^2 - 2k\omega u_0 + k^2 u_0^2 + i\eta_i k^2 \omega - ik^3 \eta_i u_0 - \mu = 0 \quad (7)$$

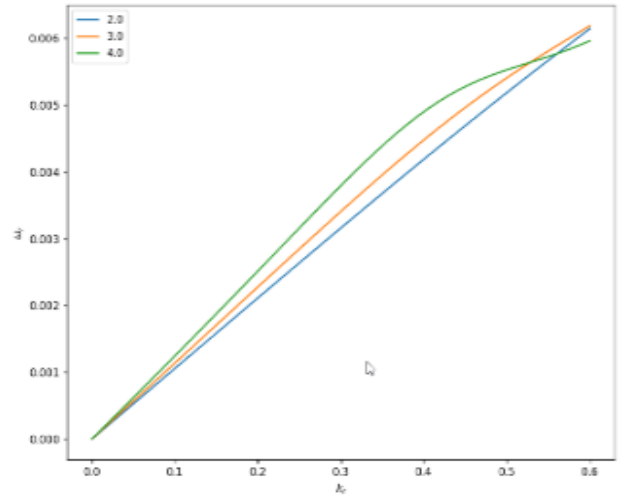


Fig. 1: Real part of dispersion relation for different η in ion-acoustic mode

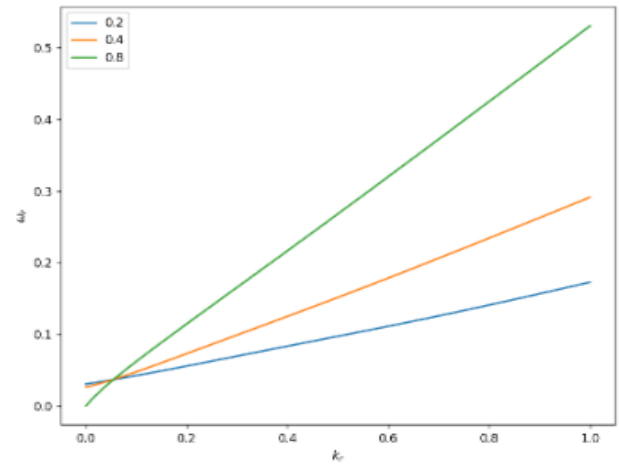


Fig. 2: Imaginary part of dispersion relation for different η in ion-acoustic mode

b) In electrostatic mode:

$$\mu \frac{\left[(\omega - u_0 k)^2 - i\eta_i k^2 (\omega - u_0 k) \right]}{\left[(\omega - u_0 k)^4 + \eta_i^2 k^4 (\omega - u_0 k)^2 \right]} - \frac{1}{k^2 \left(A + \frac{H^2 k^2}{4} \right)} = 1 \quad (8)$$

Now we will plot this to obtain the dispersion characteristics (Figure 3).

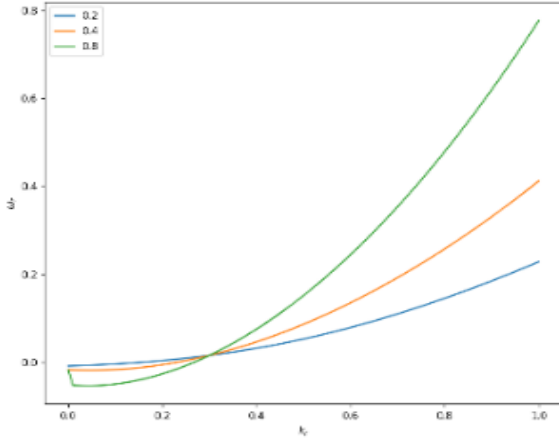


Fig. 3: Real part of dispersion relation for varying H in ion-acoustic mode

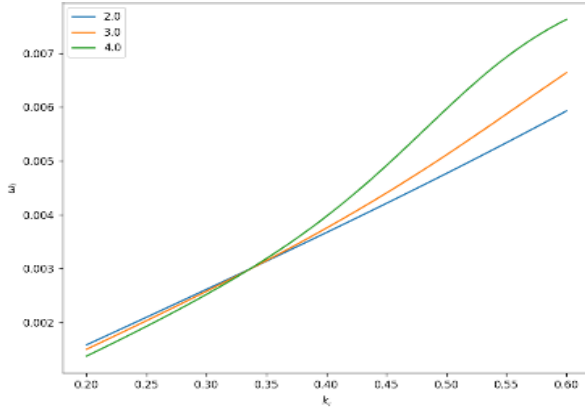


Fig. 4: Imaginary part of dispersion relation for different H in ion-acoustic mode

We have used the following stretching,

$$\xi = \delta^{1/2} (x - V_0 t); \tau = \delta^{3/2} t; \eta_i = \delta^{1/2} \eta_0 \quad (8)$$

In obtaining the KdV-Burgers equation. We use the standard reductive perturbation technique and substituting the equations (6) and (8) in the set of normalised equations for each of ion acoustic and

electrostatic waves, the equation that we get after eliminating $u_e^{(2)}$, is given by,

$$\frac{\partial(\varphi^{(1)})}{\partial\tau} + N\varphi^{(1)} \frac{\partial\varphi^{(1)}}{\partial\xi} + D \frac{\partial^3\varphi^{(1)}}{\partial\xi^3} - R \frac{\partial^2\varphi^{(1)}}{\partial\xi^2} = 0 \quad (9)$$

$$\text{Where, } N = \frac{3}{2} \frac{\mu}{(V_0 - u_0)}; D = \frac{(V_0 - u_0)^3}{2\mu}; R = \frac{\eta_0}{2}$$

$$\frac{\partial\varphi^{(1)}}{\partial\tau} + N\varphi^{(1)} \frac{\partial\varphi^{(1)}}{\partial\xi} + D \frac{\partial^3\varphi^{(1)}}{\partial\xi^3} - R \frac{\partial^2\varphi^{(1)}}{\partial\xi^2} = 0 \quad (10)$$

$$\text{Where } N = \frac{3\mu}{2(V_0 - u_0)} - \frac{(V_0 - u_0)^3}{6A^2\mu}$$

$$D = \frac{\left[1 - \frac{H^2}{4A^2} \right] (V_0 - u_0)^2}{2\mu}; R = -\frac{\eta_0}{2}$$

In equations (9) and (10) if the viscosity coefficient term η_0 vanishes, equations reduce to a normal KdV equation. Solving the KdVB equation, we have got the following solution in both cases,

$$\varphi = \frac{12D}{N} [1 - \tanh^2(\psi)] - \frac{36R}{15N} \tanh(\psi) \quad (11)$$

But, due to the difference in the values of N, D and R they are different in electrostatic and ion-acoustic modes.

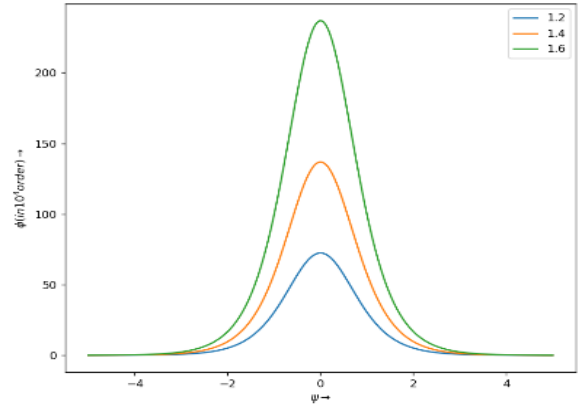


Fig. 5: Solution of KdVB equation in ion-acoustic mode for different V_0

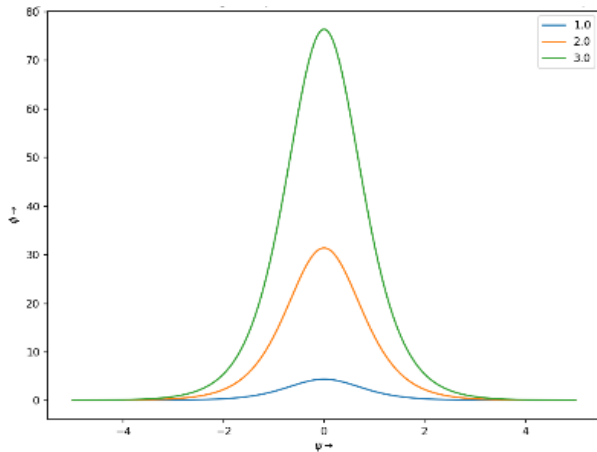


Fig. 6: Solution of KdVB equation for different V_0 in electrostatic mode and $\eta_0 = 10$

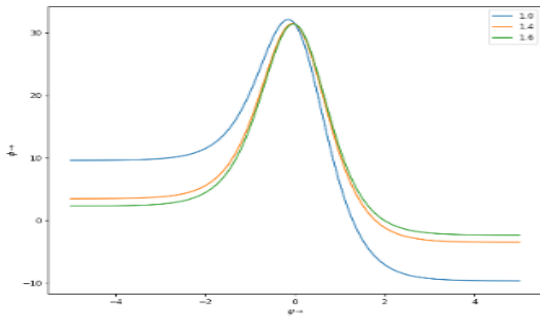


Fig 7: Solution of KdVB equation for different V_0 in electrostatic mode and $\eta_0 = 100000$

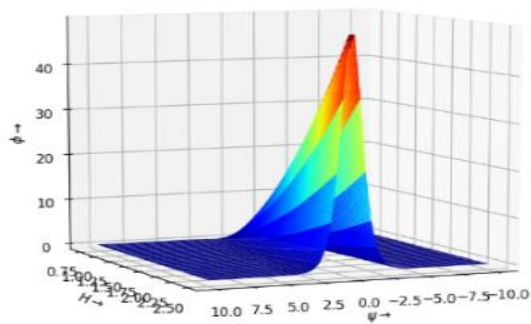


Fig. 8: Solution of KdVB equation for variable H and $\eta_0 = 10$

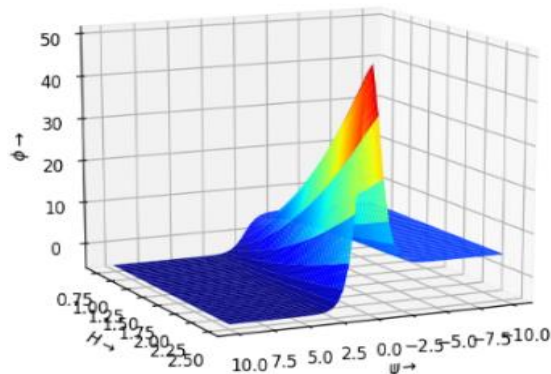


Fig. 9: Solution of KdVB equation for variable H and $\eta_0 = 100000$

We have also plotted the corresponding 3D parametric plots of the same. Now we are going to transform the KdVB equation to a NLSE equation and analyse the stability of the amplitude modulated waveform obtained from the equation. Here, we have obtained the complex NLSE of 1st type form the equation (9) as,

$$i \frac{\partial \varphi_1^{(1)}}{\partial \theta} + P \frac{\partial^2 \varphi_1^{(1)}}{\partial \rho^2} = Q \varphi_1^{(1)} \varphi_1^{(1)} \varphi_1^{(1)*} \quad (12)$$

Where,

$$P = -(3Dk + iR)$$

$$Q = N^2 k \left[\frac{1}{c} + \frac{1}{6Dk^2 + 2ick} \right]$$

Since,

$$P^* Q < 0$$

We get a waveform which is an unstable rogue wave. Now we try inserting a periodic forcing term to the RHS of KdVB equation in electrostatic mode to study the effect of external perturbations. Accordingly the KdV-Burgers equation under the action of external force is given by,

$$\frac{\partial \varphi^{(1)}}{\partial \tau} + N \varphi^{(1)} \frac{\partial \varphi^{(1)}}{\partial \xi} + D \frac{\partial^3 \varphi^{(1)}}{\partial \xi^3} = f_0 e^{i\omega\tau} \quad (13)$$

Solving this we get,

$$\varphi = \varphi_m \operatorname{sech}^2 \left(\frac{\xi - V(\tau)\tau}{W(\tau)} \right) \quad (14)$$

Where,

$$\varphi_m(\tau) = \frac{3V(\tau)}{N} \text{ And, } W(\tau) = 2\sqrt{\frac{V(\tau)}{D}}$$

These above parameters express the dependence of amplitude and width of the Forced KdV on time, mathematically.

Plotting this in 3D for $N=6$ and $D=1$ we get,

Fig. 10: ϕ plotted against ξ for varying f_0 in forced KdV equation

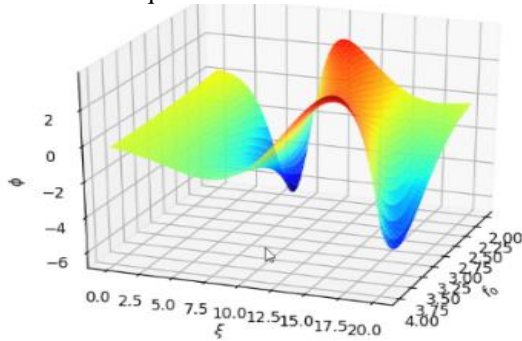
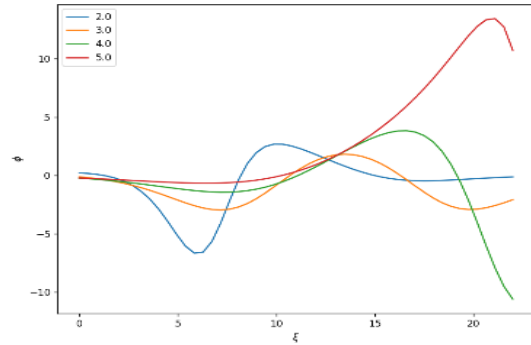


Fig. 11: ϕ plotted against ξ for different values of f_0



4. Results and Discussions

In this section, we analyse both linear and non-linear properties of two-component plasma and formation of solitary and shock profile both for ion acoustic and electrostatic mode using the standard reductive perturbation technique and including Rogue-wave study and expanded our work for Forced K-dv Equation. Now Fig (1) a more or less linear relationship between frequency and real wavenumber for different values of η It is clear that with further increase in η the graph becomes steeper. Fig 2 shows the exponential variation of the wave frequency with imaginary wave number.

This is because with increase in η wavelength decreases hence we observe an increase in wave number, consequently frequency increases. Fig (3) shows 3D real dispersion relation for different values of H. Here, it is evident that a system with larger H achieves the asymptotic value earlier than the one with lower H value. Hence, it can be said that the real dispersion relation corresponds to stable modes with increasing value of H. In Fig.(4) we find the imaginary dispersion relation between the wave frequency ω and k_i in 2D for different values of H. This shows linearity for small value of H and with higher value of H it shows asymptotic behaviour. From this linear dispersion relations clearly shows that real dispersion is a stable mode where imaginary dispersion relation relates damping hence dissipation of energy due to viscous drag.

From Fig (5) the solitary profile (symmetric) of KdVB equation i.e. ϕ is plotted against ψ for different values of phase transition velocity in ion acoustic mode it is clear that both amplitude and

width of the solitary profile increases with increase in V_0 . The high potential profile is prominent here. For electrostatic wave, when ϕ is plotted against ψ for variable values of V_0 and value is comparable to that of N and D then, we obtain a solitary as well as a shock profile as in fig. (6) and (8). We get an initial solitary profile for low value of η but as we increase the value of η it gets transformed to a shock profile. Here, the amplitude of graph increases but not so much for a very large increase in η value. However, the width increases. We have also plotted the 3D projections corresponding to solitary and shock profile in Fig. 7 and Fig. 9, respectively. From this study it is self-evident the solitary wave structure is formed due to a delicate balance between dissipative and non-linear effects.

It is shown that the plasma under consideration can support only refractive solitary waves under certain restricted regions of plasma parameters. We can conclude that the solitary and shock profile study illustrate that these behaviours are entirely governed by the movement of ions. It is evident that for larger dissipation the shock becomes more prominent and the profile becomes steeper. From the rogue wave study of our governing equations it is impossible to get stable wave solution and hence we did not continue the rogue wave study with these equations. We found many instabilities in the corresponding plots so we neglected them.

We have also obtained a solution for forced KdV equation and used some simplified parameters to plot them because they include external periodic forcing term, making our work more realistic. From Fig (10) it is clear that, the solution contains both compressive and rarefactive components. Thus, we can say that the solution can evolve into a compressive (positive amplitude of ϕ) one, starting from its rarefactive counterpart (negative amplitude of ϕ). It also shows that midpoint of the soliton shifts from left (lower ξ value) to right (higher ξ value) as f_0 increases. The same result has been

reported in [4]. However, we have confirmed it for our dataset. For simplicity we have taken $N=6$ and $D=2$. The 2D projection of the same is given in Fig (11). Finally, we have solved the forced KdV equation and plotted the result in Fig 8-9. These are the results we have obtained from our studies.

5. Application of such plasma in comet tails

A comet has two tails—the blue plasma tail and the red dust tail (or Type 1 (ion) tail and Type 2 (dust) tail). The plasma tail is caused by an interaction between the solar wind and the cometary plasma, while the dust tail is by the solar radiation pressure to the cometary dust.

Type I tails of active comets are straight, narrow plasma tails ($10^7 - 10^8$ km) and within few degrees, always point away from the sun. ‘Biermann’ postulated the existence of a continuous “solar corpuscular radiation” (solar wind) of density $n_{sw} = (1000\text{cm}^3)$ and velocity ($u_{sw} = 1000$ km/s) that represents particle flux 500 times larger. Irregularities occur due to collisional coupling between radially outward plasma flows from sun and newly ionised cometary particles.

Type II tails are broad and curved dust tails that lag behind sun-comet line. Assuming that dust grains have more or less constant mass density ρ_d , the anti-sunward radiation pressure is inversely proportional to heliocentric distance (d_h) and proportional to cross section of dust grain (πa^2), $F_{rad} \propto d^2/d_h^2$ and sunward pointing gravitational force $F_{grav} \propto a^3/d_h^3$.

Dust acoustic (DA) waves evolving into shocklets are investigated in the comet Halley plasma system relaxing to Maxwellian, Kappa, and Cairns distributions. Here, dynamics of dust is described by the fully nonlinear continuity and momentum equations. A set of two characteristic wave nonlinear equations is obtained and numerically solved to examine the DA solitary pulse that develops into oscillatory shocklets with the course of time such as at time $\tau=0$, symmetric solitary pulses are formed, which develop into oscillatory shocklets. The vector of the axis direction of the plasma tail is a sum of the vector of the solar wind velocity and the anti-vector of the orbital velocity of the comet. Consequently, the value of its deviation from the extended radius vector of the comet can serve for determining the solar wind velocity in that area of interplanetary space, where the comet is located. The characteristic feature of plasma tails is their

complex structure. In the tails, plasma condensations, rays, ring structures, archwise perturbations of the tail, and wavy formations are often observed. The complete or partial separation of the plasma cometary tails is rather frequently observed. The model used usually regarded the cometary ionized tail as a plasma cylinder and the related magneto-hydrodynamic (MHD) effects were considered. The MHD waves are excited by the Kelvin-Helmholtz (K-H) instability. In the head of the comet, the contact plane of discontinuity (i.e. the ionopause) between pure cometary plasma and the polluted solar wind plasma is unstable. Therefore, the interplanetary magnetic field wrapping around the cometary atmosphere can flow into the contact plane of discontinuity but not form a magnetic cavity [11]. After the discovery [12] of a magnetic field-free cavity around the nucleus of Comet Halley by the have been shown that such a magnetic field distribution might result from a balance between the magnetic force $\mathbf{J} \times \mathbf{B}$ and the neutral-ion drag. We may take into account the effects of dissociative recombination and mass loading arising from photo-ionisation and reached the conclusions that the Halley ionopause and its adjacent ionospheric layer with a thickness of $\sim 100\text{km}$ may possibly remain unstable, although the growth rate is substantially reduced due to recombination. The stability analysis by McKenzie et al. (1990) is extended to include the effects of degenerate finite temperature plasma pressure; the results demonstrate that plasma pressure reduces the instability growth rate of the cavity. Then the stability analysis of a cometary ionosphere is extended to include the effects of plasma motion where we can arrive at the conclusion that the cometary ionopause cannot be at rest.

6. Conclusions

It is evident that for larger dissipation the shock becomes more prominent and the profile becomes steeper. It also shows how the soliton structure converge into a shock profile. The present investigation might be helpful, in understanding the basic features of electrostatic waves in super dense astrophysical objects like white dwarfs, neutron stars as well as in the future intense laser-solid plasma experiments where the relativistic electron degeneracy effects become important. Further inclusion of magnetic field and higher order perturbation expansion will make the work more realistic. However, it will be easier to use some

simulation techniques to study Non-linear differential equations of this kind rather than analytical method.

Acknowledgements

The authors would like to thank the reviewers for their valuable inputs towards upgrading the paper. Authors would like to thank the Institute of Natural Sciences and Applied Technology, the Physics departments of Jadavpur University and Government General Degree College at Kushmandi for providing facilities to carry this work.

References

- [1] L. G. G. F. Haas and J. Goedert, "Quantum ion-acoustic waves," *Physics of Plasmas*, vol. 364, 09 2003.
- [2] B. Ghosh, S. Chandra, and S. Paul, "Amplitude modulation of electron plasma waves in a quantum plasma," *Physics of Plasmas*, vol. 18, pp. 012–106, 01 2011.
- [3] S Chandra, B.Ghosh and S N Paul, "Electron-acoustic solitary waves in a relativistically degenerate quantum plasma with two-temperature electrons," *Astrophysics and Space Science*, vol. 343, pp. 213–219, 01 2013.
- [4] S. El-Tantawy, A. Salas, M. Hammad, S. Ismaeel, D. Moustafa, and E. I. El-Awady, "Impact of dust kinematic viscosity on the breathers and rogue waves in a complex plasma having kappa distributed particles," *Waves in Random and Complex Media*, pp. 1–21, 12 2019.
- [5] S. Chandra, J. Goswami, J. Sarkar, and C. Das, "Analytical and simulation studies of forced kdv solitary structures in a two-component plasma," *Journal of the Korean Physical Society*, vol. 76, pp. 469–478, 03 2020.
- [6] J. Goswami, S. Chandra, and B. Ghosh, "Shock waves and the formation of solitary structures in electron acoustic wave in inner magnetosphere plasma with relativistically degenerate particles," *Astrophysics and Space Science*, vol. 364, 04 2019.
- [7] L.-Z. Liu, Y.-H. Ma, and J.-C. Shi, "Instability of the cometary plasma tail- the instability in a plasma sheet," *Research in Astronomy and Astrophysics*, vol. 11, no. 5, pp. 617–624, apr 2011. [Online]. Available: <https://doi.org/10.1088/1674-4527/11/5/011>
- [8] S. Borysenko, Y. Sizonenko, I. Luk'yanyk, O. Ivanova, A. Voit-sekhovskaya, T. Sergeeva, and A. Golovin, "Physical conditions in the plasma tail of comet c/1987 p1 bradfield," *Kinematics and Physics of Celestial Bodies*, vol. 27, pp. 92–97, 04 2011.
- [9] J. Goswami, S. Chandra, and B. Ghosh, "Shock waves and the formation of solitary structures in electron acoustic wave in inner magnetosphere plasma with relativistically degenerate particles," *Astrophysics and Space Science*, vol. 364, no. 4, p. 65, 2019.
- [10] J. Goswami, S. Chandra, J. Sarkar, and B. Ghosh, "Electron acoustic solitary structures and shocks in dense inner magnetosphere finite temperature plasma," *Radiation Effects and Defects in Solids*, vol. 175, no. 9-10, pp. 961–973, 2020
- [11] Ip, W. H., & Axford, W. I. 1982, "Theories of physical processes in the cometary comae and ion tails" *Comets. (A83-13376 03-90)* Tucson, AZ, University of Arizona Press, p. 588-634, 1982.
- [12] Neubauer, F. M., et al. "First results from the Giotto magnetometer experiment at comet Halley" *Nature*, 321, 352, 1986,

Received: 18th October 2020

Accepted (revised version): 22nd December 2020